



## Transition of mechanisms underlying the rate effects and its significance



Pan Xiao<sup>a,\*</sup>, Jun Wang<sup>a</sup>, Rong Yang<sup>a</sup>, Fujii Ke<sup>b</sup>, Yilong Bai<sup>a</sup>

<sup>a</sup>LNM, Institute of Mechanics, Chinese Academy of Sciences, Beijing 100190, China

<sup>b</sup>School of Physics and Nuclear Energy Engineering, Beihang University, Beijing 100191, China

### ARTICLE INFO

#### Article history:

Received 18 September 2014

Received in revised form 28 October 2014

Accepted 31 October 2014

#### Keywords:

Strain rate effect

Molecular dynamics

Thermal activation model

Potential landscapes

### ABSTRACT

The strain rate dependency of materials' failure has been widely observed in experiments and simulations, yet its microscopic mechanism is still elusive due to the complexity of failure processes. In this work, modified molecular dynamics simulations are carried out to investigate the strain rate effect over a wide strain rate range. The results demonstrate three typical failure modes induced by the competition of two timescales involved. The transition of mechanisms underlying these failure modes is discussed with a simplified model. The corresponding analysis indicates that the thermal activation model offers a good prediction for the variation of failure strain with respect to applied strain rate for failure mode I; the coupled evolution of atomic motions and potential landscapes governs the failure mode II; and the failure mode III is a result of the rapid separation between loading and deformation parts of the sample.

© 2014 Elsevier B.V. All rights reserved.

### 1. Introduction

The strain rate effect of materials, namely increase of yield stress and strength of materials with an increase in the strain rates, is a key feature in impact and shock dynamics as well as a long standing problem in materials science [1]. The effect has been widely observed in experiments of metals and alloys [2–4]. Experimental results were obtained from different techniques [4–6], such as conventional compressive/tensile testing, split Hopkinson pressure bar, shock-determined Hugoniot elastic limit stresses and femtosecond laser pulses [6], over a wide strain rate range from  $10^{-4}$  to almost  $10^9$   $s^{-1}$ . Several constitutive models had been proposed to describe the strain, stress and strain-rate relations [7–9]. However, a complete description of the dependency for different materials over such a wide strain rate range is an extremely difficult task. Various mechanisms were introduced to explain the relationship at different strain rate range. For example, it is generally known that for many metals, the dependence of flow stress sharply increases when the strain rate of deformation exceeds about  $10^3$ – $10^4$   $s^{-1}$  which is interpreted as the consequence of the change in mechanism [10]. Mechanisms such as dislocation generation, deformation twinning, and adiabatic shear banding were proposed to explain the dependency [11,12]. All these mechanisms are very important in understanding the phenomena related to the strain rate effect. However, since most of them are phenomenological

explanations, a microscopic or molecular understanding of the effect will provide us new information about basic mechanisms and governing factors.

Molecular dynamics (MD), with its ability to trace the dynamic process of each molecule, has become an orthodox method in elucidating microscopic mechanisms for mechanical behaviors of materials. Lots of MD simulations have been carried out to investigate the strain rate effect of nanoscale structures [13–17]. Besides demonstrating results similar to that observed in experiments, these simulations compensated results at ultrahigh strain rates (above  $10^9$   $s^{-1}$ ) and revealed much more details such as the evolution of structures at nanoscale. However, the simulated strain rates are limited to be very high, usually above  $10^8$   $s^{-1}$  [18]. This limitation is attributed to the intrinsic time scale of femtoseconds in MD, so it is hard to conclude that mechanisms proposed from simulation can be simply extended to that obtained from experiments with strain rates far below  $10^8$   $s^{-1}$ . Although efforts have been made to construct multi-timescale or accelerated MD methods [19,20], currently they are not mature for mechanism analysis of strain rate effect. On the other hand, due to the massive degree of freedom and complexity of potential functions, it is hard to quantitatively analyze the strain rate dependency of characteristic stress/strain based on simulation results or applying existing theoretical models, e.g. the thermal activation-strain rate analysis, to the simulation results [8]. Moreover, a deeper understanding of the effect at molecular level can also provide us some helpful clues for designing new multi-timescale methods that may compensate the current MD methods.

\* Corresponding author. Tel.: +86 10 82543930.

E-mail address: [xiaopan@lnm.imech.ac.cn](mailto:xiaopan@lnm.imech.ac.cn) (P. Xiao).

In this work, we focus on MD simulations to simple atomic systems in order to obtain results with strain rate as low as  $10^2 \text{ s}^{-1}$  which is close to that measured in experiments. Based on the evolution of atomic motion and potential landscapes, microscopic mechanisms that govern the strain rate effect are discussed. Moreover, competition of multiple timescales involved in the rate effect is also presented.

## 2. Computational framework

MD simulations were performed on 1-dimensional (1D) atomic chains and 2-dimensional (2D) atomic planes, as illustrated in Fig. 1. These configurations were chosen for two reasons. First, since MD simulations at lower strain rates are quite time consuming, simple configurations make it possible to perform simulations under a wider strain rate range. For example, it takes about one month to simulate the tensile process of an atomic chain containing only 28 atoms under a strain rate of  $10^2 \text{ s}^{-1}$  on a PC with single CPU (Intel® Core™ i7-3820QM). Unfortunately, the time-related simulation cannot be further accelerated by parallel computation, because adjacent MD steps cannot be performed on different CPUs concurrently. Therefore, if 3-dimensional (3D) atomic systems were considered, the strain rate has to be beyond  $10^8 \text{ s}^{-1}$  for a tolerable duration which does not meet the requirements for study over wide strain rate range in our work. Second, since we focus on the mechanism of strain rate effect, a simpler system will be enough to reveal the concise physics.

The atomic chain shown in Fig. 1(a) consists of 28 atoms with 4 fixed at each end. The initial length ( $l_0$ ) is 7.033 nm with interatomic distance  $d = 0.2605 \text{ nm}$ . The 2D atomic configuration in Fig. 1(b) represents a close-packed planar crystal with one of its close-packed directions parallel to the  $x$  axis. Size of the plane is  $20.64 \times 7.74 \text{ nm}$  along the  $x$  and  $y$  directions with the lattice constant  $c = 0.258 \text{ nm}$ . As illustrated, the origin of coordinate system for both 1D and 2D configurations is located at the geometric center.

The interatomic interaction is modeled using the Lennard–Jones (L–J) potential

$$\phi = 4e_0 \left[ \left( \frac{r_0}{r} \right)^{12} - \left( \frac{r_0}{r} \right)^6 \right], \quad (1)$$

with  $e_0 = 0.4912 \text{ eV}$  and  $r_0 = 0.23276 \text{ nm}$  [21]. The cutoff radius  $r_{cut}$  is set to be  $0.7 \text{ nm}$ . To reduce the influence of fixed atoms, the length of fixed ends for both atomic chain and plane is chosen to be greater than  $r_{cut}$ . Since the L–J potential parameters are fitted for copper, the atomic mass  $m$  is set to be  $63.546 \text{ g/mol}$  in simulations. Actually, embedded-atom method (EAM) potentials are

commonly used to model metals and alloys, because they usually predict better results than simple pair wise potentials. In this work, the L–J potential is used for two considerations. First, L–J potentials can also properly model metallic systems even with some defects, such as dislocations, surfaces and interfaces [22]. On the other hand, the failure of atomic systems is an energy competition process (kinetic energy and barriers between different states) which can be investigated using either L–J or EAM potentials. Second, the simple form of L–J potential is suitable for theoretical analysis which will help us extract meaningful physical parameters governing the strain rate effect.

The 1D and 2D systems were firstly equilibrated at a specific initial temperature ( $T_0$ ) to a stress-free state. Then velocity-controlled loadings were applied. Specifically, a tensile loading is implemented by applying a velocity distribution  $v_b x_b / l_0$  to the boundary atoms (where  $x_b$  denotes the position of boundary atoms), so the nominal tensile strain rate ( $\dot{\epsilon}$ ) is  $v_b / l_0$ . During simulations, boundary atoms move with the given velocity and the other atoms follow MD steps without any velocity rescaling. Physical quantities (for example, the total energy, temperature and so on) in simulations are extracted by means of time-average statistics. For example, the total resultant force on atoms of the left-side boundary  $F_L$  is averaged to characterize the tensile response of the system. Since the yield criterion for most metals is based on the maximum shear stress [23], shearing simulations of the 2D system with a periodic boundary condition imposed along the  $x$ -axis under different strain rates are also considered. For shearing simulations, the velocity distribution is applied on boundary atoms along the  $y$ -axis.

## 3. Results

Tensile simulations of the atomic chain were performed under strain rates ranging from  $4.28 \times 10^2$  to  $1.0 \times 10^{12} \text{ s}^{-1}$ . Boundary force  $F_L$  versus tensile strain  $\epsilon_t$  with typical strain rates is plotted in Fig. 2 and three failure modes can be identified.

- (1) Smooth elastic stage followed by a catastrophic fracture, e.g. tensile curves for strain rate of  $1.13 \times 10^4$  and  $1.62 \times 10^7 \text{ s}^{-1}$ , respectively. In the former case, the atomic chain breaks at 5.46%, which is hereafter denoted by the failure strain  $\epsilon_f$ . With the strain rate increasing to  $1.62 \times 10^7 \text{ s}^{-1}$ ,  $\epsilon_f$  is enhanced to 6.53%. Observations on fractured atomic configurations show that most of the samples break at regions far away from fixed ends. This failure mode is detected as strain rates are below  $10^9 \text{ s}^{-1}$ .

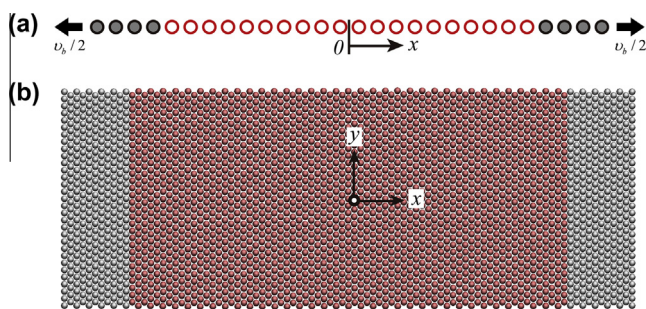


**Fig. 1.** Configuration for an atomic chain (a) under tensile loading and an atomic plane and (b) used for 2D tensile and shearing simulations. Red atoms are free to move, while boundary atoms (in gray) are manipulated by external velocities. (For interpretation of the references to color in this figure legend, the reader is referred to the web version of this article.)

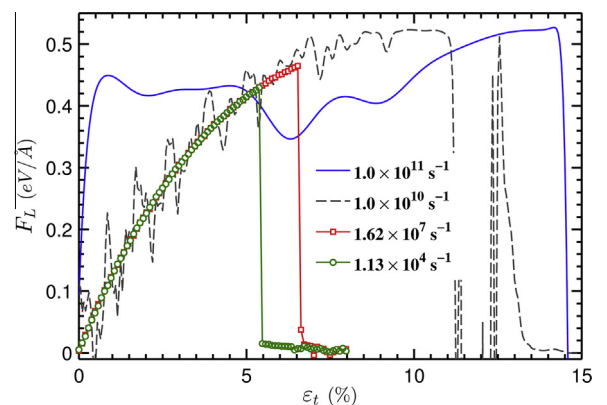


**Fig. 2.** Variation of boundary forces with tensile strain for atomic chains under various strain rates.

Download English Version:

<https://daneshyari.com/en/article/7959793>

Download Persian Version:

<https://daneshyari.com/article/7959793>

[Daneshyari.com](https://daneshyari.com)